IMMUNOLOGY

Blockade of IL-7 signaling suppresses inflammatory responses and reverses alopecia areata in C3H/HeJ mice

Zhenpeng Dai[1], Eddy Hsi Chun Wang[1], Lynn Petukhova[1], Yuqian Chang[1], Eunice Yoojin Lee[1], Angela M. Christiano[1,2]*

Copyright © 2021 The Authors, some rights reserved; exclusive licensee American Association for the Advancement of Science. No claim to original U.S. Government Works. Distributed under a Creative Commons Attribution NonCommercial License 4.0 (CC BY-NC).

The interleukin-7 (IL-7) signaling pathway plays an important role in regulation of T cell function and survival. We detected overexpression of IL-7 in lesional skin from both humans and C3H/HeJ mice with alopecia areata (AA), a T cell–mediated autoimmune disease of the hair follicle. We found that exogenous IL-7 accelerated the onset of AA by augmenting the expansion of alopecic T cells. Conversely, blockade of IL-7 stopped the progression of AA and reversed early AA in C3H/HeJ mice. Mechanistically, we observed that IL-7Rα blockade substantially reduced the total number of most T cell subsets, but relative sparing of regulatory T cells (T_{regs}). We postulated that short-term anti–IL-7Rα treatment in combination with a low dose of T_{reg}-tropic cytokines might improve therapeutic efficacy in AA. We demonstrated that short-term IL-7Rα blockade in combination with low doses of T_{reg}-tropic cytokines enhanced therapeutic effects in the treatment of AA, and invite further clinical investigation.

INTRODUCTION

Alopecia areata (AA) is a chronic inflammatory disease that attacks the hair follicle (HF) (*1*–*4*); however, the etiology and pathogenesis of AA remain incompletely understood. AA is a T cell–mediated autoimmune disease involving the collapse of HF immune privilege, which develops because of genetic and environmental factors leading to cytotoxic $CD8^+$ T cell activity, cytokine release, and apoptosis of the HF (*4*–*6*). We recently identified $CD8^+NKG2D^+$ T cells as the key pathogenic cells in AA, which guided our investigation of the cytokines that drive their activation and function (*5*, *6*). Our transcriptional profiling analysis revealed that the γc cytokines interleukin-2 (IL-2), IL-7, and IL-15 were up-regulated in lesional skin from both humans and C3H/HeJ mice with AA (*6*). Blockade of either of IL-2 or IL-15 using antibodies (Abs) prevented the development of AA in the C3H/HeJ skin-grafted model (*6*); however, the role of IL-7 in AA remains undefined.

IL-7 plays an important role in immune system development and homeostasis by promoting lymphoid cell growth and survival (*7*–*9*). The effect of IL-7 on T cells is controlled by the expression of the IL-7 receptor (IL-7R) complex (composed of the γ chain and IL-7Rα), as well as by the state of differentiation of the T cell and the availability of the cytokine IL-7 itself (*7*–*9*). In addition to the critical role of IL-7 in naïve and memory T cell growth and survival, recent research also revealed that IL-7 enhances the function and expansion of interferon-γ (IFN-γ)–producing T helper type 1 (T_H1) cells (*10*). IL-7 plays a key role in the pathogeneses of multiple T cell–dependent autoimmune diseases, including multiple sclerosis (MS), type 1 diabetes (T1D), rheumatoid arthritis (RA), and Sjögren's syndrome (SS) (*8*). Therefore, a therapeutic strategy aimed at blocking the IL-7 signaling pathway may prevent or reverse the autoimmune disorders in mouse models of these diseases (*10*–*12*).

We and others previously showed that AA exhibits a notable IFN gene expression signature in lesional skin from both humans and C3H/HeJ mice with AA (*3*, *6*). IFN-γ may contribute to the collapse of HF immune privilege by up-regulating major histocompatibility complex (MHC) class I expression in the HF and inducing apoptosis of the HF (*13*). Here, we demonstrated that IL-7 is up-regulated in lesional skin from both humans and C3H/HeJ mice with AA. We investigated the role of IL-7 in the development and onset of AA in the C3H/HeJ mouse model and found that IL-7 enhances the cytotoxic T cell type 1 (Tc1) immune response in C3H/HeJ mice. We demonstrated that blockade of IL-7Rα reduces the number of alopecic T cells yet relatively spares regulatory T cells (T_{regs}), leading to the reversal of AA. Furthermore, we found that anti–IL-7Rα treatment in combination with low dose of T_{reg}-tropic cytokines (such as IL-2 and IL-33) enhanced its therapeutic benefit in the treatment of AA without severe T cell depletion. Together, we defined a previously unidentified role of IL-7 in the development of AA and revealed critical underlying disease mechanisms for disease resolution. These findings provide evidence that therapeutic approaches blocking IL-7 signaling alone or in combination with T_{reg}-tropic cytokines may represent a promising new combination therapy in the treatment of human AA.

RESULTS

Increased expression of IL-7/IL-7Rα pathway in AA lesional skin

IL-7 is primarily produced by stromal cells of lymphoid tissues and bone marrow, as well as other tissues including the intestine, liver, and skin (*14*, *15*). We observed a higher level of IL-7 expression in lesional skin from C3H/HeJ mice with AA (C3H AA) than in skin from C3H/HeJ mice without hair loss (C3H NC) (Fig. 1, A and B), consistent with our previous transcriptomic analysis (*6*). In the periphery, IL-7 is an important factor in regulating immune cell survival and function (*7*, *8*). As previously shown, high percentages of $CD8^+$ T cells were detected in the lesional skin from C3H AA compared with C3H NC mice (*6*). We observed that skin-infiltrating $CD8^+$ T cells expressed comparable amounts of IL-7Rα compared to $CD8^+$ T cells in skin-draining lymph nodes (SDLNs) and spleen (Fig. 1, C and D). Other immune cell types, including B cells and NK cells, lacked expression of IL-7Rα (fig. S1A) (*8*, *9*). In human

[1]Department of Dermatology, College of Physicians and Surgeons, Columbia University, New York, NY 10032, USA. [2]Department of Genetics and Development, Vagelos College of Physicians and Surgeons, Columbia University, New York, NY 10032, USA. *Corresponding author. Email: amc65@cumc.columbia.edu

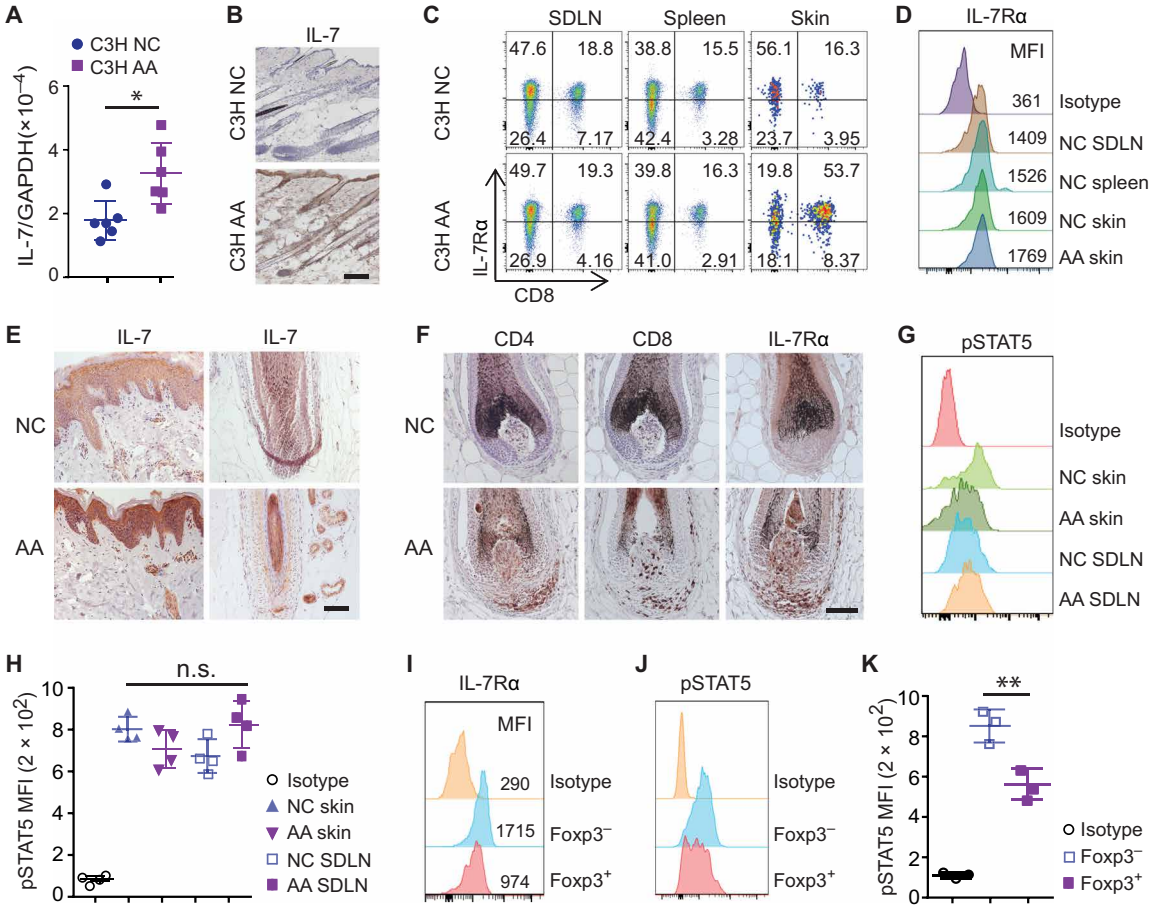

Fig. 1. Increased IL-7 in AA lesional skin. (**A**) Quantitative reverse transcription polymerase chain reaction measuring transcript levels of IL-7 in skin of C3H/HeJ mice with or without AA. *$P < 0.05$ (unpaired Student's t test). GAPDH, glyceraldehyde-3-phosphate dehydrogenase. (**B**) Representative immunohistochemical analyses of IL-7 protein expression in C3H/HeJ mice with or without AA. Scale bars, 100 μm. Data represented from three C3H AA and three C3H NC controls. (**C** and **D**) Representative flow cytometric analysis of IL-7Rα expression on $CD8^+$ T cells by gating $CD45^+$ cells within SDLN, spleen, or skin from C3H mice with or without AA. MFI, mean fluorescence intensity. (**E** and **F**) Representative immunohistochemical analyses of human scalp sections of AA and normal controls showing IL-7 (E) and IL-7Rα protein expression (F). Data represented from three AA and four NC controls. Scale bars, 100 μm. (**G** and **H**) pSTAT5 expression in $CD8^+$ T cells after treatment with IL-7. (G) Representative histograms. (H) Summary graphs of MFI. n.s., not significant [one-way analysis of variance (ANOVA)]. (**I**) IL-7Rα expression by $CD4^+Foxp3^-$ T cells and $CD4^+Foxp3^+$ T_{regs} within SDLN from C3H NC mice. (**J** and **K**) pSTAT5 expression in $CD4^+Foxp3^-$ T cells and T_{regs} after treatment with IL-7. (J) Representative histograms. (K) Summary graphs of MFI. **$P < 0.05$ (one-way ANOVA).

AA scalp biopsies, IL-7Rα was also detected in T cells infiltrating the HFs in which the expression of IL-7 was up-regulated (*6*), compared to HF from normal control scalp skin (Fig. 1, E and F).

We investigated the effects of IL-7–mediated signaling in skin-infiltrating T cells. Signal transducer and activator of transcription 5 (STAT5) is a key transcription factor downstream of IL-7Rα, and IL-7 requires STAT5 to induce Bcl-2 expression and to maintain effector T cells (*9*). Phosphorylation of STAT5 (pSTAT5) levels was determined in T cells following stimulation with IL-7 by using a pSTAT5-specific monoclonal Ab (mAb) and intracellular flow cytometry. We found that IL-7 drove pSTAT5 almost equally in $CD8^+$ T cells within both skin and lymphoid organs (Fig. 1, G and H), indicating that the IL-7 signaling pathway was functional in skin-infiltrating $CD8^+$ T cells. Because IL-7Rα expression is lower on T_{regs} than non-T_{regs} (Fig. 1I), IL-7 drove less pSTAT5 in T_{regs} compared to $CD4^+$ non-T_{regs} (Fig. 1, J and K) (*9*). Accordingly, B cells that lack the expression of IL-7Rα showed no detectable response to IL-7 (fig. S1B). Together, these results indicate that overexpression of IL-7 in lesional skin may enable IL-7–dependent T cells to better survive in skin.

IFN-γ increased IL-7 production in skin

Type I IFNs and IFN-γ induced IL-7 production in keratinocytes, stroma, and epithelial cells in previous studies (*16*, *17*). Because lesional skin from both patients with AA and C3H AA mice exhibited a notable IFN gene signature (*6*), we postulated that IFN-γ produced by skin-infiltrating mononuclear cells, specifically $CD8^+$ T cells, might promote local production of IL-7 in the skin. To investigate the role of IFN-γ signaling in IL-7 production, we injected recombinant mouse IFN-γ intradermally in areas of the skin of C3H NC mice (*18*). We detected up-regulation of IL-7 in the skin following IFN-γ treatment compared to phosphate-buffered saline (PBS) (fig.

S2A). Moreover, using a mAb that targets IFN-γ receptor α (IFN-γRα) to block IFN-γ signaling, we observed a significant decrease in the expression of IL-7 in the skin from anti–IFN-γRα–treated mice compared to controls (fig. S2B). These results indicate that IFN-γ signaling may promote IL-7 production in the skin under homeostasis or in the context of inflammatory conditions such as AA, which may, in turn, promote the survival of IL-7–dependent lymphocytes (*16*).

IL-7 promoted the development of Tc1 and accelerates the development of AA

IL-7 promotes T_H1 cell responses, as well as priming and inducing activation of autoreactive T cells in mouse models, such as experimental autoimmune encephalomyelitis (EAE) and nonobese diabetic (NOD) (*10*, *11*). Because AA is a T cell–mediated autoimmune disease of the HF, next, we assessed whether IL-7 influenced the development of T_H1 or Type 1 $CD8^+$ T cells (Tc1) in C3H/HeJ mice. Freshly isolated naïve $CD4^+$ T cells and naïve $CD8^+$ T cells were stimulated with anti-CD3 in the presence of IL-7. Consistent with previous reports in other models (*10*, *11*), significantly greater percentages of IFN-γ^+CD4^+ T cells and IFN-γ^+CD8^+ T cells were induced by IL-7 than PBS (Fig. 2, A and B). Cytotoxic $CD8^+$ T cells led to HF destruction through the release of cytotoxic mediators, including granzymes (GZMs) and perforin-1 (PRF1), comprising the cytotoxic T lymphocyte (CTL) gene signature that we previously defined in AA lesional skin from both human AA and C3H/HeJ AA mice (*6*). γc cytokines including IL-2, IL-15, and IL-21 are known to augment the cytotoxic function of $CD8^+$ T cells by inducing the production of those cytotoxic mediators (*19*). We observed that IL-7 also enhanced the production of GZMA, GZMB, and PRF-1 by $CD8^+$ T cells (Fig. 2, C and D).

Given the role of IL-7 in promoting T_H1 and Tc1 responses in vitro, we next evaluated the function of IL-7 in vivo by exogenous administration of IL-7 using the C3H/HeJ skin-grafted model. To extend the in vivo life span and activity of IL-7, we took advantage of a highly bioactive form of IL-7 complexed to anti–IL-7 Ab (IL-7c) with some modifications (*20*, *21*). C3H/HeJ mice were administered with IL-7c 2 weeks after skin grafting, a time point at which effector T cells begin to proliferate and accumulate in the SDLNs (*6*). We treated the mice with a lower dose of IL-7c (0.5-μg IL-7 with 5-μg mAb M25) than previous reports (1.5-μg IL-7 with 15-μg mAb M25) (*20*, *21*), for a total of two times at 7-day intervals. IL-7c–treated mice displayed faster and more severe hair loss than PBS-treated mice (Fig. 2, E and F). The role of IL-7 in accelerating AA development was further confirmed by comparing the frequencies of skin-infiltrating $CD8^+$ T cells and IFN-γ–producing $CD8^+$ T cells from IL-7c– or PBS-treated mice (Fig. 2, G and H).

We also examined the effects of IL-7 on immune cells from lymphoid organs 1 week after the last dose of IL-7c administration. In agreement with previous reports in other mouse models (*20*, *21*), IL-7c increased the total number of lymphocytes in lymphoid organs (fig. S3A). We also found that IL-7c robustly increased the frequency of $CXCR3^+CD8^+$ T cells, T-bet^+CD8^+ T cells, and IFN-γ–producing $CD8^+$ T cells in SDLNs (Fig. 2I and fig. S3B) but only slightly increased the frequency of $CD4^+$ T cell counterparts (fig. S3C). The frequency of $CD4^+$ T_{regs} in IL-7c–treated mice may have been decreased because of the low response to IL-7 stimulation (Fig. 1K and fig. S3C). Collectively, these results demonstrate that IL-7 plays a key role in the development of AA by enhancing Tc1 responses in C3H/HeJ mice.

IL-7Rα blockade prevented disease onset in in C3H/HeJ skin-grafted model of AA

We next investigated role of endogenous IL-7 in AA pathogenesis by IL-7 signaling blockade. The anti-mouse IL-7Rα (clone A7R34) Ab has been used to block IL-7Rα signaling when administered in vivo (*11*, *12*, *22*). C3H/HeJ skin-grafted mice were treated with A7R34 or isotype control starting on the day of alopecic skin grafting to induce AA. In the control group, all mice developed hair loss by 7 weeks after skin grafting. In contrast, none of anti–IL-7Rα-treated mice displayed any signs of hair loss (Fig. 3, A and B). The thymic stromal lymphopoietin (TSLP) receptor shares the IL-7Rα chain but pairs with the cytokine receptor like factor 2, rather than γc, as the second chain comprising the TSLP receptor complex (*23*). The role of the anti–IL-7Rα mAb could potentially inhibit signaling from both IL-7 and TSLP in vivo. We ruled out a potential role of TSLP in AA development by treating the C3H/HeJ skin-grafted mice with anti-TSLP neutralizing mAbs (Fig. 3, C and D) (*24*). These results indicated that endogenous IL-7 plays a pivotal role in AA development in C3H/HeJ skin-grafted mice.

IL-7Rα blockade prevented disease onset in T cell receptor retrogenic mouse model AA

Retrogenic T cell receptor (TCR) mouse models consist of bone marrow cells from a recombination activating gene 1 (RAG-1)–deficient C57BL/6 mouse transduced with a retroviral vector that carries specific TCR α and β chains, grafted into RAG-1–deficient C57BL/6 mice (*25*, *26*). Here, we adapted the previously described 1MOG244 TCR retrogenic system to induce spontaneous AA in C57BL/6 mice (fig. S4, A to C). Analysis of the T cell compartment of these mice revealed that nearly 40% of $CD8^+$ T cells coexpressed NKG2D, consistent with the central role for these cells in the C3H/HeJ mouse model of AA (fig. S4D) (*6*).

Previous studies showed that neither IFN-γ, tumor necrosis factor–α (TNF-α), nor IL-17 played a significant role in the pathogenesis of AA in the 1MOG244 TCR retrogenic mouse model (*26*). To test whether IL-7 signaling affected alopecic T cells in this mouse model, we labeled the 1MOG244 $CD8^+$ T cells from donor AA mice with CellTrace Violet before adoptive transfer into C57BL/6 RAG-1–deficient recipients, followed by anti–IL-7Rα treatment. As shown by CellTrace Violet dilution, anti–IL-7Rα markedly inhibited 1MOG244 $CD8^+$ T cell proliferation (Fig. 3E). Furthermore, anti–IL-7Rα mAb administration prevented hair loss in all treated mice, compared to control mice that all developed AA after 1MOG244 $CD8^+$ T cell adoptive transfer (Fig. 3, F and G) (*26*). Together, we demonstrated an essential role of IL-7/IL-7Rα signaling in promoting the proliferation and function of AA effector T cells in both the C3H/HeJ skin-grafted mouse model and the C57BL/6 1MOG244 TCR retrogenic model.

IL-7Rα blockade reversed early AA in C3H/HeJ mice

To evaluate the efficacy of anti–IL-7Rα in a clinically relevant context, we asked whether anti–IL-7Rα could reverse newly established disease by initiating therapy 5 to 7 weeks after skin grafting, a time point at which grafted C3H/HeJ mice begin losing hair (*6*). Notably, after 8 weeks of anti–IL-7Rα mAb administration, more than 60% of treated mice displayed hair regrowth in areas of previous hair loss, whereas all control mice developed progressive and extensive hair loss (Fig. 4, A and B). Consistent with hair regrowth in treated mice, anti–IL-7Rα substantially reduced skin inflammation shown by staining of histological markers of the disease (CD8, MHC class

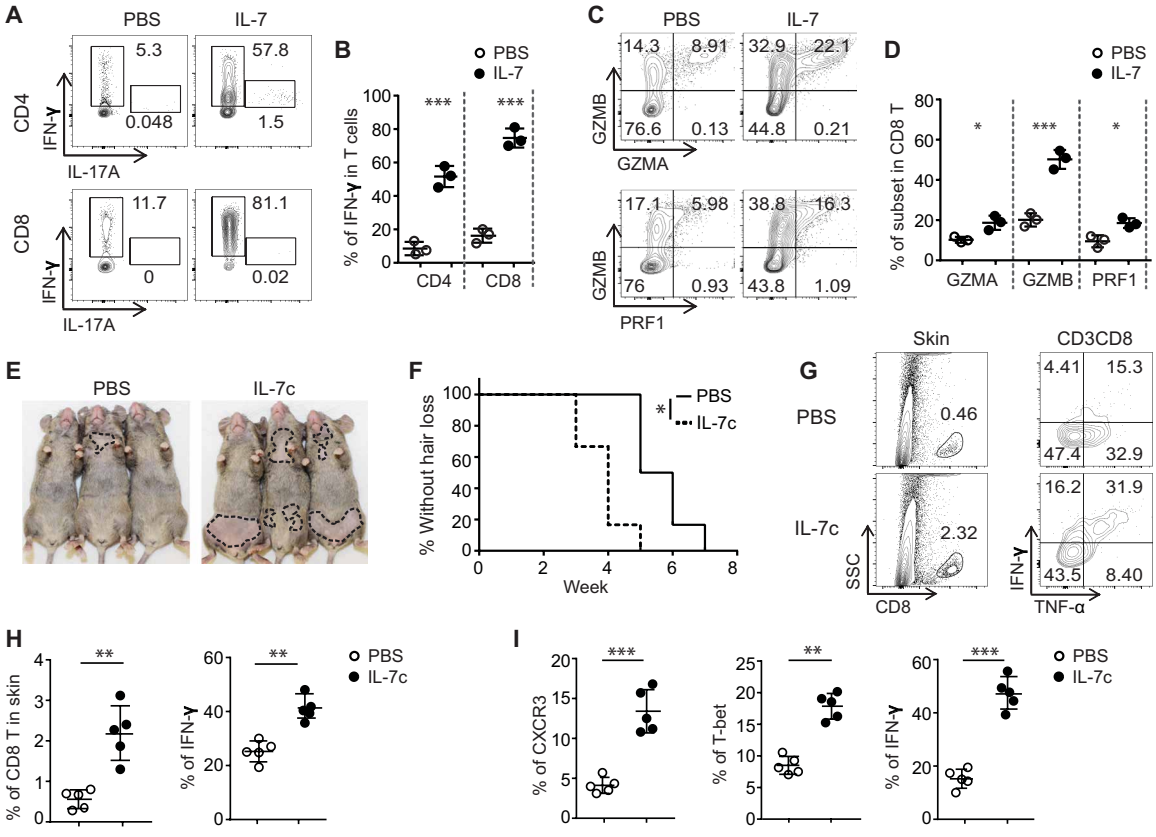

Fig. 2. IL-7 promoted the development of Tc1 cells and accelerated the development of AA. (**A** to **D**) Purified naïve CD4$^+$ and CD8$^+$ T cells were stimulated in the presence of IL-7 (10 ng/ml) for 4 days. (A and B) Representative flow cytometric plots and summary graphs of IFN-γ–producing T cells. (C and D) Representative flow cytometric plots and summary graphs of GZMA, GZMB, or PRF1–producing CD8$^+$ T cells. Data are represented as the means ± SD of three independent experiments. *P < 0.05 and ***P < 0.001 (unpaired Student's t test). (**E** and **F**) C3H skin-grafted mice were given IL-7c (0.5-μg IL-7 mixed with 5-μg anti–IL-7 mAb M25, 37°C for 20 min) once a week for 2 weeks after 2 weeks after skin grafting. Representative images (E) and the incidence of AA onset (F) in grafted C3H/HeJ mice treated with IL-7c (n = 6) or PBS (n = 6). *P < 0.05, log-rank test. (**G** and **H**) Representative fluorescence-activated cell sorting plots and summary graphs of the percentages of T cell profiles in the skin of grafted mice treated with IL-7c or PBS. Data are represented as the means ± SD of two independent experiments. **P < 0.01 (unpaired Student's t test). (**I**) Summary graphs of the percentages of CD8$^+$ T cell subsets within SDLNs. Data are represented as the means ± SD of two independent experiments. **P < 0.01 and ***P < 0.001 (unpaired Student's t test). Photo credit: Mice pictures taken by Zhenpeng Dai, Columbia University.

I, and MHC class II) (Fig. 4C). Flow cytometry analysis of skin single cell suspensions further revealed that the frequency of CD45$^+$ immune infiltrates was markedly reduced in anti–IL-7Rα–treated mice (Fig. 4D). Total CD8$^+$ T cell frequency and IFN-γ–producing CD8$^+$ T cell frequency among skin CD45$^+$ immune infiltrates were both significantly reduced in anti–IL-7Rα–treated mice (Fig. 4D). Concordantly, global analysis of skin gene expression revealed that both the IFN and CTL components of the ALADIN (Alopecia Areata Disease Severity Index) score strongly discriminated between anti–IL-7Rα–treated mice and control animals (Fig. 4, E and F). Collectively, IL-7Rα blockade reduced the number of alopecic effector T cells present and inhibited their function in affected skin, leading to disease reversal.

IL-7Rα blockade inhibited T effector cell function and favored immune regulation

We next investigated the immunological consequences of anti–IL-7Rα treatment on different T cell populations. CD8$^+$ T cells within SDLNs from anti–IL-7Rα–treated C3H/HeJ mice produced significantly less IFN-γ and IL-2 compared to controls (Fig. 5A). We next evaluated the function of effector T cells. We and others previously showed that CD8$^+$ T cells isolated from SDLNs of C3H/HeJ AA mice can induce AA in normal-haired young C3H/HeJ recipients (*6*, *27*). As expected, all recipient mice developed AA by 10 weeks after adoptive transfer of SDLN T cells from isotype-treated mice. In contrast, same number of SDLN CD8$^+$ T cells from anti–IL-7Rα–treated C3H/HeJ mice failed to induce AA during the time of observation (15 weeks after cell transfer) (Fig. 5, B and C), indicating that anti–IL-7Rα treatment suppressed alopecic effector T cells in treated mice.

Because IL-7 is a critical factor for lymphocyte survival, we next analyzed the changes in lymphocytes in SDLN and spleen after treatment. Anti–IL-7Rα treatment significantly reduced the total numbers of SDLN cells, CD3$^+$ T cells, CD4$^+$ T cells, CD8$^+$ T cells, and B cells compared to controls (Fig. 5D). Among CD8$^+$ T cells, three populations, including CD8$^+$NKG2D$^+$ T cells, CD8$^+$CD44$^+$CD62L$^-$ T cells, and IFN-γ–producing CD8$^+$ T cells, were markedly reduced in number and frequency in anti–IL-7Rα–treated C3H/HeJ mice (fig. S5, A and B) (*6*). In agreement with previous reports in other mouse models (*8*, *11*), C3H/HeJ mice treated with anti–IL-7Rα showed a significant increase in the frequency of PD-1$^+$CD44$^+$ T cells and T_{regs} within SDLNs compared to controls (Fig. 5, E to H). Despite a

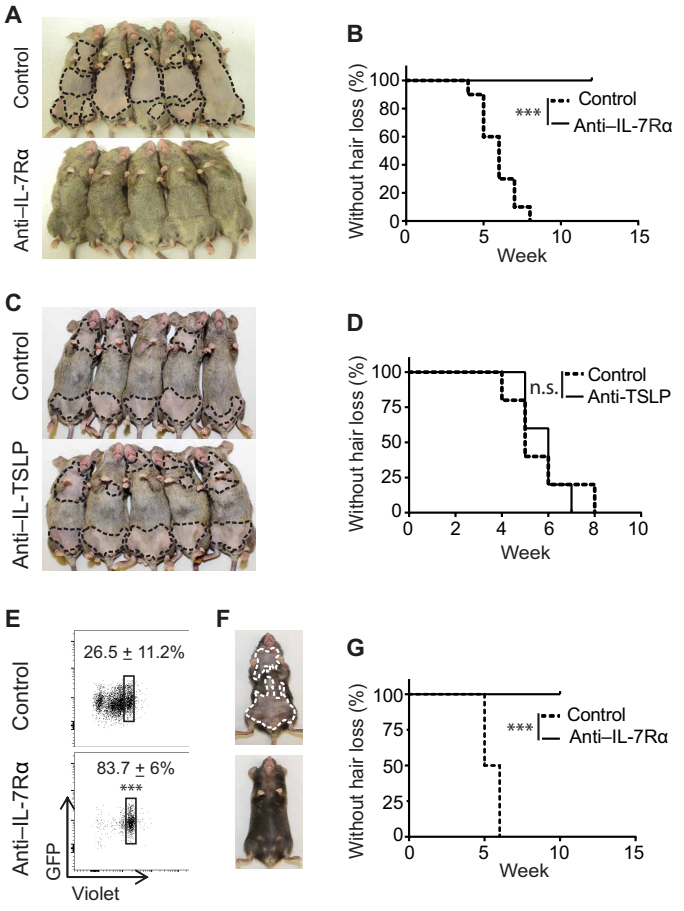

Fig. 3. IL-7Rα blockade prevented development of AA. (**A** to **D**) C3H/HeJ skin-grafted mice were treated with anti–IL-7Rα mAb, anti-TSLP mAb, or control Ab, administrated by intraperitoneal injection two times weekly for 8 weeks, beginning on the day of grafting. Representative images (A) and the incidence of AA onset (B) in skin-grafted C3H/HeJ mice treated with anti–IL-7Rα mAb ($n = 15$) or control mAb ($n = 15$) for 8 weeks. ***$P < 0.001$ (log-rank test). Representative images (C) and the incidence of AA onset (D) in skin-grafted C3H/HeJ mice treated with anti-TSLP mAb ($n = 10$) or control mAb ($n = 10$) for 8 weeks. n.s., not significant (log-rank test). (**E** to **G**) Purified $CD8^+$ T cells (3×10^6) from 1MOG244 retrogenic TCR B6 $RAG1^{-/-}$ mice were adoptively transferred to B6 $RAG1^{-/-}$ recipients, followed by anti–IL-7Rα or control mAb treatment. (E) The transferred $CD8^+$ T cells were gated on green fluorescent protein (GFP) expression, and the T cell proliferation was measured by CellTrace Violet dye dilution 1 week after treatment. ***$P < 0.001$ (unpaired Student's *t* test). Representative images (F) and the incidence of AA onset (G) in anti–IL-7Rα mAb– or control mAb–treated B6 $RAG1^{-/-}$ recipients (five mice for each group). ***$P < 0.001$ (log-rank test). Photo credit: Mice pictures taken by Zhenpeng Dai, Columbia University.

decrease in their absolute numbers, the T_{reg}/T_{eff} cell (T_{reg}/CD8) ratios were increased in the SDLNs from anti–IL-7Rα–treated C3H/HeJ mice (Fig. 5I). We also observed that the suppressive function of T_{regs} from anti–IL-7Rα–treated C3H/HeJ mice was not significantly changed when compared to T_{regs} from control Ab–treated mice (fig. S6A), indicating that the effect of anti–IL-7Rα treatment spares T_{regs}, consistent with previous reports (*11*). We observed that the expression of PD-L1 (programmed cell death 1 ligand 1) and PD-L2 were markedly up-regulated in lesional skin from C3H/HeJ AA mice compared to controls (fig. S7A), consistent with our previously published gene expression microarray data (*6*). Skin-infiltrating T cells from anti–IL-7Rα–treated C3H/HeJ mice contained a higher percentage of $PD\text{-}1^+CD8^+$ T cells than controls (fig. S7B). Moreover, the $PD\text{-}1^+CD8^+$ T cells from anti–IL-7Rα–treated C3H/HeJ mice produced less IFN-γ and TNF-α compared to controls (fig. S7C). Given the critical roles of T_{regs} and programmed cell death protein 1 (PD-1)/PD-L pathway in peripheral tolerance (*28*, *29*), we postulated that IL-7Rα blockade might favor immune tolerance in the context of AA (*8*, *11*).

We next investigated whether T_{regs} or the PD-1/PD-L pathway played a role in AA reversal after anti–IL-7Rα treatment. First, C3H/HeJ AA mice were treated with anti–IL-7Rα for 4 weeks. Then, the mice were administered either anti–PD-1 mAb (to block the PD-1 signaling pathway), or anti-FR4 (folate receptor 4) mAb (to deplete T_{regs}) (*30*, *31*). Previous reports showed that PD-1/PD-L1 blockade abrogates the protective effects of anti–IL-7Rα treatment in the NOD mouse model (*11*). However, we found that PD-1 blockade neither accelerated nor delayed disease in treated AA mice compared to controls (Fig. 5J). In contrast, following T_{reg} depletion, we observed an increase in hair loss in AA mice (Fig. 5J), indicating that an increased frequency of T_{regs} might be one of the underlying mechanisms during AA resolution following IL-7Rα blockade. Moreover, we found a protective role of T_{regs} in AA development after T_{reg} depletion in C3H/HeJ skin-grafted mice (fig. S6B). Together, these results demonstrate that IL-7Rα blockade reduced alopecic effector T cell frequency and, simultaneously, spared T_{regs} during AA resolution.

A combination of anti–IL-7Rα and low-dose T_{reg}-tropic cytokine promotes resolution of AA

Given the role of T_{regs} in controlling pathogenic autoimmune response in AA (Fig. 5O), we next compared the frequency of T_{regs} in lymphoid organs and skin in C3H/HeJ mice, with or without AA. We found that the frequency of T_{regs} increased within the SDLNs yet significantly decreased in the skin over the course of the disease (Fig. 6, A and B), suggesting that disruption of the T_{reg}/T_{eff} cell balance in the skin could be a contributing factor in AA (*32*). Manipulating T_{regs} is a promising strategy to treat autoimmunity (*33*). The T_{reg}-tropic cytokines IL-2 and IL-33 are crucial for the survival and stability of T_{regs} in vivo (*34*, *35*). Low-dose IL-2 has shown therapeutic value in the treatment of several autoimmune diseases, including a small pilot study in AA (*36*, *37*). Likewise, the cytokine IL-33 has recently been shown to expand tissue T_{regs} and to enhance their suppressive capacity in vivo (*38*). We found that neither low doses of IL-2 nor of IL-33 used in our study were able to prevent AA development in C3H/HeJ skin-grafted mice (Fig. 6, C and D), possibly because of strong inflammatory responses in AA that overcome the suppressive function of T_{regs} in alopecic skin.

Although long-term anti–IL-7Rα treatment showed efficacy in AA resolution (Fig. 4), it also had the undesirable effect of significantly reducing the total numbers of lymphocytes (Fig. 5E). Because anti–IL-7Rα treatment reduced T effectors, but relatively spared the T_{regs} (Fig. 5), we postulated that a short-term anti–IL-7Rα treatment to suppress strong inflammatory responses transiently without inducing lymphopenia, in combination with low-dose IL-2 or IL-33 to increase the frequency of T_{regs}, might promote AA resolution. We added either low-dose IL-2 or low-dose IL-33, as described in previous reports, after anti–IL-7Rα mAb administration (total of doses) (Fig. 6E) (*39*). We observed that IL-2 and IL-33 combinatorial

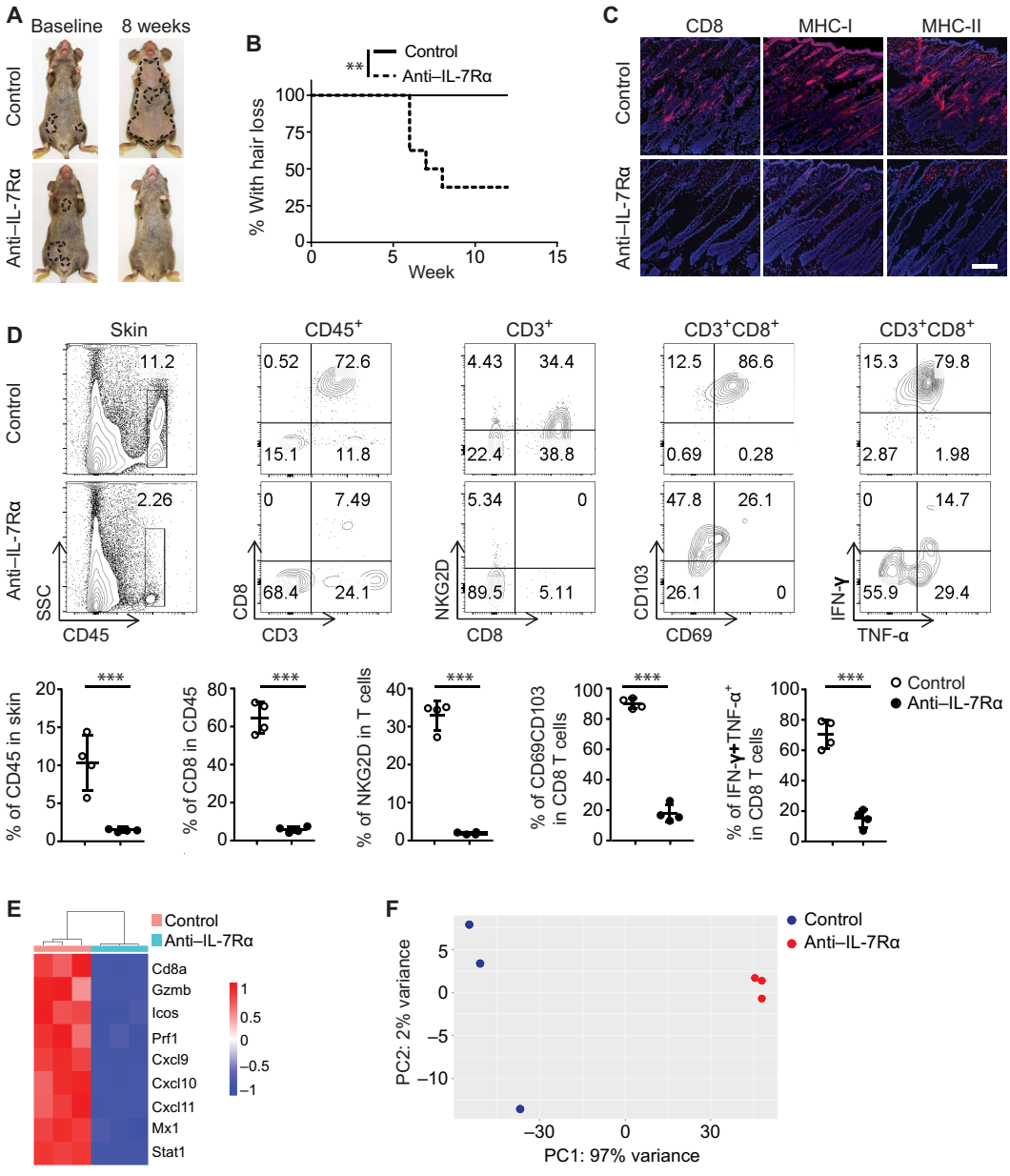

Fig. 4. IL-7Rα blockade reversed early-onset AA in C3H/HeJ mice. Four to 5 weeks after AA skin grafting, C3H/HeJ skin-grafted mice with early-onset AA were administered control mAb ($n = 10$) or anti–IL-7Rα mAb ($n = 10$) by intraperitoneal injection two times weekly for 8 weeks. (**A**) Representative images of anti–IL-7Rα or control Ab–treated C3H/HeJ mice before and after treatment. (**B**) Survival curve analysis demonstrates the hair regrowth between the two groups. $^{**}P < 0.01$ (log-rank test). (**C**) Representative immunofluorescence images of skin sections from the two groups, stained with anti-CD8, anti–MHC-I, or anti–MHC-II Abs. Scale bars, 100 μm. (**D**) Single-cell suspensions of skin cells were gated on CD45 and CD3 for flow cytometry analysis, or the cells were stimulated with phorbol 12-myristate 13-acetate/ionomycin for cytokines expression by intracellular flow cytometry. Top: Representative flow cytometric plots data showing immune cell profiles in skin of C3H/HeJ mice from the two groups. Bottom: Summary graphs of various percentages of immune cells. $^{***}P < 0.001$ (unpaired Student's t test). (**E** and **F**) RNA-seq analysis from treated mice presented as a heatmap (E) and as a cumulative ALADIN index (F). Photo credit: Mice pictures taken by Zhenpeng Dai, Columbia University.

immunotherapy did not completely reverse the AA in most treated mice (Fig. 6F). Nevertheless, the combinatorial immunotherapy increased the frequency of T_{regs} in mice skin and showed effects on slowing AA progression compared to PBS (Fig. 6, G to I), suggesting a role for T_{regs} in AA development. Our results demonstrated that short-term IL-7Rα blockade in combination with T_{reg}-trophic cytokines may have therapeutic benefit in the treatment of AA.

IL-7Rα polymorphisms and AA risk

Recently, polymorphisms in *IL-7Rα* have been shown to contribute to the susceptibilitour geneomic datay of developing autoimmune disorders in human complex diseases (*40*). In genome-wide association studies (GWAS), several IL-7Rα single-nucleotide polymorphisms were associated with autoimmune disorders, including MS, T1D, ulcerative colitis (UC), sarcoidosis, and primary biliary

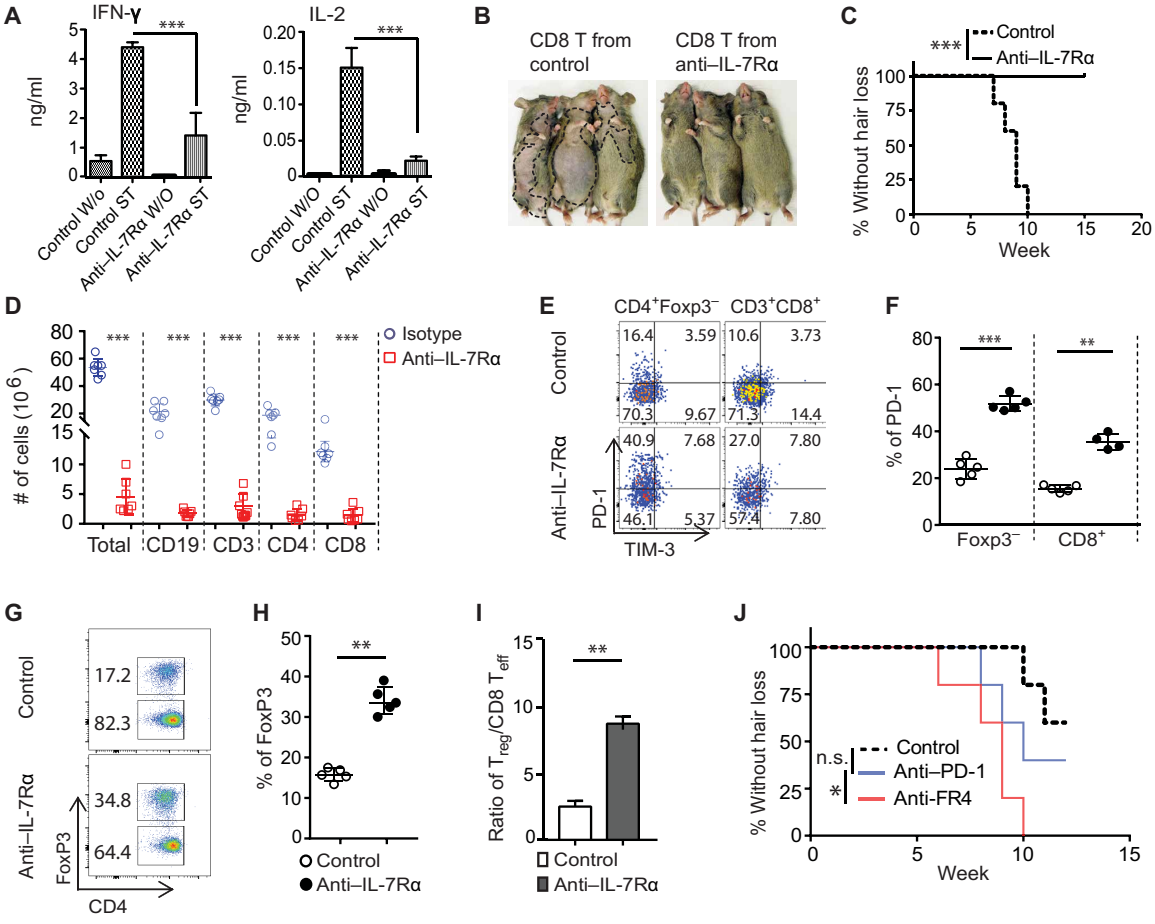

Fig. 5. IL-7Rα blockade inhibited effector T cells but spared T_{regs} in C3H/HeJ mice. (**A** to **C**) C3H/HeJ AA mice were treated as in Fig. 4. (A) Cytokines production by purified SDLN T cells after stimulation for 48 hours. ST (stimulation with anti-CD3/CD28), W/O (without stimulation). ***$P < 0.001$ (one-way ANOVA). (B and C) Normal C3H/HeJ mice ($n = 6$) were transferred with 10×10^6 activated $CD8^+$ T cells (either from anti–IL-7Rα or control mAb–treated mice). Representative images (B) and the incidence of AA (C). ***$P < 0.001$ (log-rank test). (**D** to **I**) The animals were treated as in Fig. 4. (D) The total numbers of immune cell subsets within SDLNs of the anti–IL-7Rα or control mAb–treated mice. (E to F) Representative flow cytometric plots and summary graphs of the percentages of PD-1^+ T cells within indicated T cell populations. (G to H) Representative flow cytometric plots and summary graphs of the percentages of T_{regs} within total $CD4^+$ T populations. (I) Bar diagram depicts the ratio of T_{regs}:$CD8^+$ T effectors within SDLNs from the two groups. Data are represented as the means ± SD of two independent experiments. **$P < 0.01$ (unpaired Student's t test). (**J**) The incidence of AA onset in C3H/HeJ mice were treated with anti–IL-7Rα mAb following treatment with anti–PD-1 mAb ($n = 10$), T_{reg} depletion ($n = 10$), or control mAb ($n = 10$). ns, not significant; *$P < 0.05$, log-rank test. Photo credit: Mice pictures taken by Zhenpeng Dai, Columbia University.

cirrhosis (PBC) (*40*). However, the mechanisms by which these variations alter risk of disease remain to be elucidated. To ask whether the IL-7 pathway has relevance in human AA, we reanalyzed our previous GWAS data in AA (*5*), we found that one single-nucleotide polymorphism (rs6891096) in the IL-7Rα region showed a nominal AA association ($P = 0.000717$) (fig. S8A). Moreover, we found that the production of IFN-γ by T cells stimulated by IL-7 was higher from patients compared to control subjects (fig. S8B). This suggests that IL-7 may reduce the threshold for activation of alopecic T cells, under a predisposed genetic background, leading to AA progression s.

DISCUSSION

Previous studies proposed that disequilibrium between the production of proinflammatory cytokines and anti-inflammatory cytokines could be involved in the persistence of AA (*1*, *2*). The lack of targeted therapies for AA can be attributed in part to an incomplete understanding of the cytokine pathways that underlie AA pathogenesis (*42*, *43*). In RA and psoriasis, for example, the identification of proinflammatory cytokines critically involved in pathogenesis led to effective therapies using blocking Abs to interrupt these signaling pathways necessary for sustained inflammatory responses in tissue, such as TNF-α and IL-17A, respectively (*44*, *45*). In this study, we demonstrated the critical role of IL-7 in AA by showing that (i) IL-7 is highly up-regulated in AA lesional skin; (ii) administration of exogenous IL-7 accelerated the onset of AA; and (iii) blockade of IL-7 signaling by administrating anti–IL-7Rα mAb ameliorated ongoing AA and reversed established AA.

In agreement with our previous gene expression studies, we showed that both humans and C3H/HeJ mice with AA show up-regulated expression of IL-7 in lesional skin. IFNs drive several proinflammatory pathways that facilitate pathogenic recognition and activation of adaptive and innate responses, including the

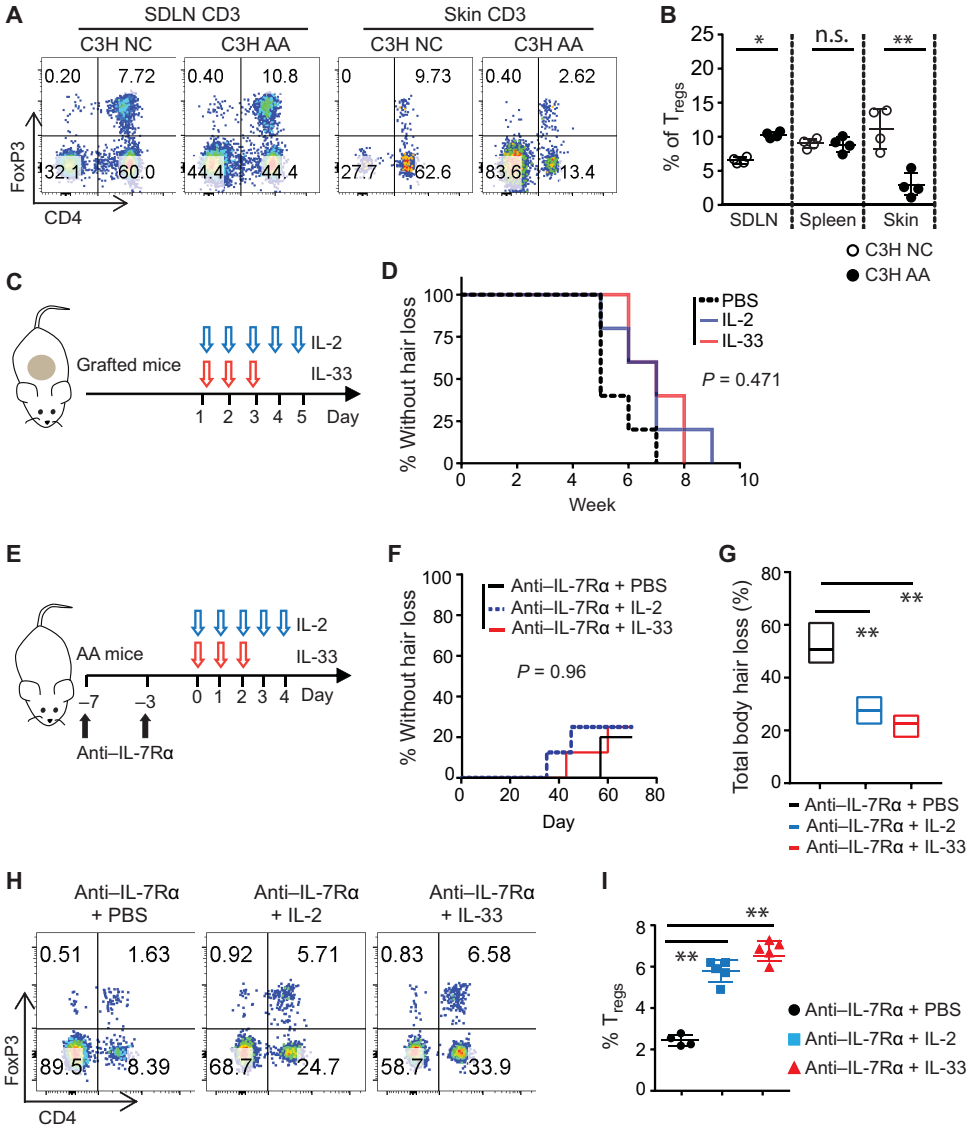

Fig. 6. Combined treatment of anti–IL-7Rα and low-dose IL-2 or IL-33 increases the percentage of T_{regs} in C3H/HeJ AA mice. (**A**) Flow cytometric analysis of the percentage of $CD4^+Foxp3^+$ T_{regs} in the total $CD3^+$ T cell population of the SDLNs, spleen, and skin. Representative flow cytometric plots from a 15-week-old nongrafted C3H/HeJ mouse and a same aged new-onset C3H/HeJ AA mouse are shown. (**B**) The graph is a summary of $CD4^+Foxp3^+$ T_{regs} in the total $CD3^+$ T cells in SDLNs, spleen, and skin of nongrafted and grafted C3H/HeJ AA mice. Data are represented as the means ± SD. ns, not significant; $^*P < 0.05$ and $^{**}P < 0.01$ (unpaired Student's *t* test). (**C** and **D**) C3H/HeJ skin-grafted mice were treated with IL-2 or IL-33, administrated by intraperitoneal injection, beginning the day of grafting. (C) Schematic diagram showing the experiment design. (D) The incidence of AA onset in grafted C3H/HeJ mice treated with IL-2 ($n = 5$), IL-33 ($n = 5$), or PBS ($n = 5$). $P = 0.471$ (log-rank test). (**E** to **I**) C3H/HeJ mice with AA were treated with anti–IL-7Rα mAb for 1 week, after which IL-2, IL-33, or PBS were then administrated by intraperitoneal injection. (E) Schematic diagram showing experiment design. (F) Survival curve analysis depicts the hair regrowth after treatment. $P = 0.96$ (log-rank test). (G) Total body hair loss of C3H/HeJ AA mice after treatment. $^{**}P < 0.01$ (one-way ANOVA). (H) Representative flow cytometric plots showing $CD4^+$ T_{regs} within the total $CD3^+$ T cell population in the skin after treatment. (I) Summary graphs of the percentages of $CD4^+$ T_{regs} within T cell populations (right). $^{**}P < 0.01$ (one-way ANOVA).

recruitment of immune effectors through the induction of chemokines (*46*). The role of IFN-γ in AA was previously established using knockout studies and pharmacological administration of cytokines that precipitated disease (*47*). IL-7 promotes T_H1 responses, as well as priming activation of autoreactive T cells in several mouse models of autoimmune diseases, including EAE, T1D, and SS (*8*, *10*–*12*, *22*). We asked whether IL-7 plays a role in the enhanced T_H1 responses and IFN-γ production in AA. We showed that IL-7 accelerated the development of AA and increased the number of IFN-γ–producing T cells infiltrating the HFs. IL-7 is mainly produced by stromal cells in lymphoid tissues and bone marrow, and other tissues including skin are also known sites of IL-7 production (*15*). It was previously reported that IFN-γ induces expression of IL-7 in keratinocytes (*48*). To this end, we showed that treatment with IFN-γ increased the expression of IL-7 in the skin, and likewise, blockade of IFN-γ signaling pathway decreased the expression of IL-7 in the skin. This

result revealed a positive feedback regulation between the IFN-γ and IL-7 signaling cascades in the skin (*16*).

IL-7 is an important factor in the regulation of T cell survival and function, and IL-7 as well as its receptor are involved in T cell–dependent autoimmune processes (*8*). The role of the IL-7/IL-7Rα pathway in autoimmune diseases is underscored by several recent studies demonstrating that IL-7Rα blockade in the EAE and NOD mouse models had therapeutic benefit (*10*, *11*). To define the role of IL-7 in the pathogenesis of AA, we found that therapeutic anti–IL-7Rα treatment in C3H/HeJ AA mice induced hair regrowth and reversed early disease. Furthermore, anti–IL-7Rα treatment reduced inflammation and markedly reduced skin infiltration by T cells. T cells from mice treated with anti–IL-7Rα produced less IFN-γ and IL-2 and did not induce AA in C3H/HeJ recipients as effectively as T cells from isotype control–treated mice, indicating that IL-7 is critical for the functioning of T effector cells in AA. Our results showed that the efficacy of anti–IL-7Rα mAbs is associated with the induction of lymphodepletion. However, the IL-7 biology in C3H/HeJ mouse model and other rodent models shows differences from that in primates and humans, because administration of high doses of anti–IL-7Rα antagonistic mAb has not been reported to induce lymphopenia in primates and in human phase 1 trial (*49*, *50*).

In the NOD mouse model, IL-7Rα blockade not only reduced the number of activated effector T cells but also involved the up-regulation of PD-1 and signaling via its ligand PD-L1, leading to long-term tolerance as shown (*11*). PD-1/PD-L has been implicated as a critical pathway for peripheral tolerance (*51*). PD-L expression is often elevated in response to tissue insult and inflammation, and PD-1 is overexpressed on effector T cells (*51*). This may represent the "last hope" of the tissue or organ as it attempts to regulate self-destructive T cells. Although PD-1–ligand expression is increased in the HF of C3H/HeJ mice with AA, the disease still develops, suggesting a defect in this signaling pathway in stopping disease progression. We showed that IL-7Rα blockade reverses the onset of AA with a concomitant increase in the expression of PD-1 on T cells in C3H/HeJ mice. PD-1 blockade did not significantly accelerate AA. However, we cannot exclude a role for the PD-1/PD-L signaling pathway in AA, because this pathway is significantly up-regulated in AA lesional skin. Our data are consistent with previous reports in other mouse models of disease in which the role of the PD-1 signaling pathway may become less prominent because IL-7Rα blockade induces multiple mechanisms of action for disease resolution (*52*).

T_{regs} are central to maintain immunological self-tolerance and immune homeostasis by suppressing aberrant or excessive immune responses (*32*, *33*), and T_{reg} defects contribute to the loss of tolerance in human autoimmune diseases and mouse models (*53*). We observed that the ratio of T_{reg}/T_{eff} cells significantly decreased in the skin of C3H/HeJ mice over the course of the AA. Enhancing T_{reg} is one strategy to treat autoimmune diseases. IL-2 is a key survival factor for T_{regs}, and low-dose IL-2 therapy has been used in clinical trials for several autoimmune diseases (*37*). However, the efficacy of low-dose IL-2 in human AA treatment was not clear. IL-33 is an IL-1 family cytokine that signals via ST2, and IL-33/ST2 signaling is known to expand tissue-resident T_{regs} and increase their immunomodulatory function in several mouse model of inflammatory disorders (*54*). Low-dose IL-33 has not been reported in the treatment of AA. Our results suggest that anti–IL-7Rα treatment depleted most effector T cells and increased the relative frequency of T_{regs}, which then play a role in AA recovery. However, we found that low-dose IL-2 or low-dose IL-33 alone used in our study was not effective in the treatment of C3H AA, perhaps because of the strong inflammatory responses in AA. Because long-term anti–IL-7Rα mAb treatment induces broad lymphodepletion, we postulated that a short-term anti–IL-7Rα treatment without inducing lymphopenia, in combination with low-dose IL-2 or IL-33, might have greater efficacy in disease reversal. We found that low-dose IL-2 or IL-33 combined with IL-7Rα blockade augmented the frequency of T_{regs} with skin, and this combination treatment showed some efficacy in halting disease progression, but it did not completely reverse AA in most treated mice. We observed that a short-term anti–IL-7Rα treatment suppresses the action of effector T cells only transiently, possibly because of the ability of IL-15 and/or other compensatory gamma chain cytokines that provide "back-up" support for the alopecic CD8 T cells (*6*). Previous reports in other disease models showed that disease protection by IL-2 is highly dose dependent (*34*). Our results suggest the need for careful evaluation of the dose of trophic cytokines used to expand T_{regs} avoiding unintended exacerbation of the alopecic T cell response within the skin. T_{reg} instability has been reported in NZW mice (*35*). T_{regs} in peripheral lymphoid organs in C3H mice did not show wide differences in proportions with other inbred strains of mice [except for New Zealand white mice (NZW)], when compared with the published data (Fig. 6B) (*35*). We also showed that C3H mouse T_{regs} displayed strong suppression in vitro, as well as sensitivity to trophic cytokines in our study. These results suggest T_{reg} functioning normally in C3H/HeJ mice.

In summary, we demonstrated that IL-7 plays an important role in the pathogenies of AA and that IL-7Rα blockade, in combination with a low dose of IL-2 or IL-33, may represent a promising new therapeutic candidate in the treatment of AA. Further investigation needed to determine whether anti–IL-7Rα leads to active tolerance as a mechanism of AA reversal.

MATERIALS AND METHODS

Study design

The objectives of the present study were to examine the role of IL-7 in the development of AA and to determine whether blocking IL-7 signaling could prevent or reverse disease in mouse model of AA. For our study, AA was established by either skin grafting, adoptive T cell transfer, or TCR retrogenic T cell transfer. Experiments were designed to validate cytokines (including IL-2, IL-7, and IL-33) or mAbs (including anti–IL-7Rα, anti-TSLP, anti–PD-1, anti-FR4, and isotype mAbs) in disease prevention or acceleration. On the basis of preliminary experiments and a type I error (α) = 0.05, we calculated that a minimum of five mice per group were required for statistical significance for our prevention and treatment studies for 80% power to detect an effect in at least 50% of animals included in each experiment. The primary outcome variable between two groups was hair loss. Calculations were performed using G*Power software. Mouse hair status was recorded after each treatment. The number of mice per experimental group and the number of repetitions of the experiments are indicated in the individual figure legends.

Mice

C3H/HeJ and B6.129S7-*Rag1*^{tm1Mom}/J (Rag1$^{-/-}$ B6) mice were obtained from the Jackson laboratory and maintained under specific pathogen–free conditions. Experiments were performed in

compliance with institutional guidelines as approved by the Institutional Animal Care and Use Committee of Columbia University.

Generation of C3H/HeJ AA mice

We used two different methods to induce AA in C3H/HeJ mice, including skin grafting and adoptive T cell transfer from SDLN, both of which were described previously (*6*). For the skin graft model, a piece of skin (1-cm diameter) from a C3H/HeJ donor mouse with extensive AA was grafted onto the dorsal back skin of 8- to 10-week-old C3H/HeJ recipients and covered with a bandage for 10 days. For adoptive T cell transfer, 5 million magnetic bead (MACS, Miltenyi Biotec)–purified $CD8^+$ T cells isolated from SDLN were transferred intradermally into normal-haired young C3H/HeJ recipients (*6*). Hair status was examined twice weekly.

Generation of 1MOG244.1 TCR retrogenic mice

1MOG244.1 TCR retroviral vectors and GP+E-86 (American Type Culture Collection) producer cell lines were generated according to previous studies (*25*, *26*). Briefly, $Rag1^{-/-}$ B6 mice were administrated 5-fluorouracil (Sigma-Aldrich) (150 mg/kg body weight). After 3 days, bone marrow cells were harvested and pooled together and cultured in complete Dulbecco's modified Eagle's medium (DMEM) with 20% fetal calf serum (FCS) supplemented with recombinant murine IL-3 (20 ng/ml; PeproTech), recombinant human IL-6 (50 ng/ml; PeproTech), and recombinant murine stem cell factor (SCF) (50 ng/ml; PeproTech) for 24 hours at 37°C in 5% CO_2. The bone marrow cells were infected with TCR-expressing retrovirus in the presence of polybrene (6 μg/ml; Sigma-Aldrich) through spin-based transduction (1000*g* for 60 min at 37°C) for consecutive three times, and the cells were left to rest for an additional 48 hours in complete DMEM with 20% FCS supplemented with IL-3, IL-6, and SCF. The transduced bone marrow cells were injected into sublethally irradiated $Rag1^{-/-}$ B6 mice (450 rad) at a ratio of one recipient mouse per two bone marrow donors through retro-orbital injections. For adoptive T cell transfer disease, 2 million magnetic bead (MACS, Miltenyi Biotec)–purified $CD8^+$ T cells isolated from SDLN and spleen were transferred intravenously into $Rag1^{-/-}$ B6 mice. Hair status was examined twice weekly.

Antibodies

We performed flow cytometric staining with fluorophore-conjugated Abs that were obtained from BioLegend, BD Biosciences, and Thermo Fisher Scientific. Abs used in the experiments with mouse cells included anti-CD3 (17A2), anti-CD4 (GK1.5), anti-CD8 (53-6.7), anti-CD11b (M1/70), anti-CD11c (N418), anti-CD19 (1D3), anti-CD25 (PC61), anti-CD44 (IM7), anti-CD45 (30-F11), anti-CD49b (DX5), anti-CD62L (MEL-14), anti-CD69 (H1.2F3), anti-CD103 (2E7), anti-FR4 (12A5), anti-NKG2D (CX5), anti-NKp46 (29A1.4), anti-TCRγδ (GL3), anti-F4/80 (BM8), anti–PD-1 (29F.1A12), anti–TIM-3 (B8.2C12), GZMA (3G8.5), anti-GZMB (GB11), anti–PRF1 (S16009A), anti–T-bet (4B10), anti-FOXP3 (FJK-16 s), anti–IL-2 (JES6-5H4), anti–IL-17A (eBio17B7), anti–TNF-α (MP6-XT22), and anti–IFN-γ (XMG1.2). Abs used in the experiments with human cells included anti-CD3 (HIT3a), anti-CD4 (OKT4), anti-CD8 (HIT8a), anti–IFN-γ (4S.B30), and anti–IL-13 (JES10-5A2).

Flow cytometry and fluorescence activated cell sorting

Single-cell suspensions were stained with fixable, viability live/dead Fixable Blue (Thermo Fisher Scientific) in PBS for 15 min at room temperature, after which they were washed twice with RPMI 1640 with 10% fetal bovine serum (FBS). Nonspecific Ab binding was blocked using mouse or human TruStain FcX (BioLegend). For surface marker staining, Abs were diluted at 1:200 and incubated with cells in BD brilliant stain buffer (BD Biosciences) on ice for 30 min. For intracellular staining, the cells then were fixed and permeabilized using a FOXP3 staining kit (Thermo Fisher Scientific) for detection of FoxP3, T-bet, GZMA, GZMB, PRF-1, IL-13, IL-17A, TNF-α, or IFN-γ, according to the FoxP3 staining protocol from the manufacturer. Viable cell populations were gated on the basis of forward and side scatters and by Fixable Blue staining and acquired with a BD LSR II flow cytometer (BD Biosciences). Analysis was carried out using FlowJo software (TreeStar).

For cell sorting, cells were incubated with fluorochrome-conjugated Abs in staining buffer (PBS with 2% FBS), on ice for 20 min. The samples were run on an Influx cell sorter (BD Biosciences). Viable cell populations were gated on the basis of forward and side scatters and 4′,6-diamidino-2-phenylindole (DAPI) staining (BioLegend). The viability and purity of sorted cells were greater than 95%.

Preparation of single-cell suspensions

SDLNs or spleens were homogenized and filtered through a 70-μm cell strainer. Splenocytes were depleted of erythrocytes by RBC Lysis Buffer (Thermo Fisher Scientific). After the mice were euthanized, hair was removed using hair clippers. Skin was then defatted and digested in 0.25% trypsin for 20 min at 37°C. Epidermis was separated from the dermis using forceps and scalpel blades. The dermis was finely minced and digested for 45 min at 37°C with collagenase type IV (1 mg/ml; Worthington) and deoxyribonuclease I (0.05 mg/ml; Sigma-Aldrich) in RPMI 1640 with 5% FBS in a shaker. Digested skin was homogenized, filtered through a 70-μm cell strainer, and washed before staining or stimulation.

Cell culture and stimulation

All cells were cultured in RPMI 1640 supplemented with 10% FCS, 4 mM GlutaMAX, 20 mM Hepes, 0.05 mM 2-mercaptoethanol, penicillin (1000 U/ml), and streptomycin (1 mg/ml) (all from Thermo Fisher Scientific). Purified $CD4^+$ T cells or $CD8^+$ T cells were stimulated with Dynabeads mouse T-activator CD3/CD28 (Thermo Fisher Scientific) at a bead-to-cell ratio of 2:1 for 4 days in the presence of recombinant murine IL-7 (10 ng/ml) (PeproTech) for T_H1 or Tc1 cell induction in 24-well plates (Corning). To detect intracellular cytokines, cells were restimulated with eBioscience Cell Stimulation Cocktail (Thermo Fisher Scientific) for 5 hours plus eBioscience Protein Transport Inhibitor Cocktail (Thermo Fisher Scientific). To detect IFN-γ and IL-2 production, T cells were stimulated with Dynabeads mouse T-activator CD3/CD28 for 2 days. The production of IFN-γ or IL-2 was measured by an enzyme-linked immunosorbent assay kit (BioLegend).

T_{reg} suppression assays

$CD25^{high}CD4^+$ T_{regs} and $CD8^+$ T cells were isolated from mice SDLNs on an Influx cell sorter (*30*). The $CD8^+$ T cells were labeled with 2.5 μM CellTrace Violet (Thermo Fisher Scientific), cultured with the T_{regs} at various ratios, and stimulated with plated-bound anti-CD3 (1 μg/ml) (145-2C11; Bio X Cell) and anti-CD28 (2 μg/ml) (37.51; Bio X Cell) in a flat-bottom 96-well plate (Thermo Fisher Scientific) for 4 days. The effector T cells were gated on CD8,

and the percent suppression was calculated according to previous reports (*55*).

Phosphorylation assays

Single-cell suspensions were incubated with recombinant murine IL-7 (20 ng/ml; PeproTech) at 37°C for 20 min. The cells were subsequently fixed with 4% paraformaldehyde in PBS for 15 min at room temperature. Fixed cells were permeabilized with 90% ice-cold methanol for 30 min on ice, washed once, and stained with cell surface markers (CD45, CD3, CD4, CD8, and CD25) and anti–phospho-STAT5 (C71E5, Cell Signaling Technology) for 2 hours at room temperature. The cells were acquired with a BD LSR II flow cytometer (BD Biosciences), and analysis was carried out using FlowJo software (Treestar).

In vivo treatment

For IL-7 induction studies, C3H/HeJ mice (without AA) received a single intradermal injection of 400 ng recombinant murine IFN-γ (PeproTech) in the areas of the back skin, and PBS was used as a control. After 48 hours, skin biopsies were taken. C3H/HeJ mice (without AA) received an injection of 200-μg anti–IFN-γRa (GR-20; Bio X Cell) or isotype control immunoglobulin G (IgG) (Bio X Cell) by intraperitoneal injection two times weekly for 4 weeks. For IL-7 stimulation in vivo, C3H/HeJ grafted mice were given IL-7c [0.5-μg recombinant murine IL-7 mixed with 5-μg anti–IL-7 mAb (M25; Bio X Cell), 37°C for 20 min], once a week for 2 weeks after 2 weeks after skin grafting. The preparation of IL-7/M25 complex was described as previously (*20*).

For AA prevention studies, treatment was started at the day of grafting (using the C3H/HeJ grafted model) or adoptive T cell transfer (using the retrogenic TCR C57BL/6 model). Anti–IL-7Rα mAb (A7R34; Bio X Cell), anti-TSLP (28F12; BioLegend), or isotype control IgG (Bio X Cell) was administrated by intraperitoneal injection (250 μg) two times weekly for 6 to 8 weeks. In separate experiment recombinant human IL-2 (PeproTech) was administered at 25,000 U per dose ip daily for 5 days (*39*); or recombinant murine IL-33 (BioLegend) was administered at 2 μg per dose ip daily for 3 days (*39*).

For AA reversal studies, anti–IL-7Rα mAb (A7R34; Bio X Cell) or isotype control IgG was administered into early-onset AA mice (5 to 7 weeks after skin grafting) by intraperitoneal injection (500 μg) two times weekly for 8 weeks. For Ab combination treatment, early-onset AA mice were treated anti–IL-7Rα mAb (500 μg) two times weekly for two to 4 weeks, after which anti–PD-1 (RMP1–14; Bio X Cell) was administered at 200 μg per dose intraperitoneally (ip) twice per week for 3 weeks or anti-FR4 (TH4; BioLegend) was administered at 200 μg per dose ip twice per week for 2 weeks. For cytokine combination treatment, AA mice were treated anti–IL-7Rα mAb (500 μg) two times for 1 week, after which recombinant human IL-2 (PeproTech) was administered at 25,000 U per dose ip daily for 5 days; recombinant murine IL-33 (BioLegend) was administered at 2 μg per dose ip daily for 3 days.

Immunofluorescence and immunohistochemistry

Immunofluorescence and immunohistochemical staining of mice skin sections were performed as previously described (*6*, *18*). Skin tissues were embedded in OCT (Optimal Cutting Temperature) compound (Sakura). Skin sections (8 μm) were incubated with primary Abs listed below in PBS + 5% donkey serum (Vector Laboratories) blocking buffer for 1 hour at room temperature. After incubation with rat anti-CD8 (53-6.7, BioLegend), rat anti–I-A/I-E (M5/114.15.2, BioLegend), biotin mouse anti–H-2KK (36-7-5, BioLegend), or goat anti-mouse IL-7 (R&D Systems) overnight at 4°C, followed by ImmPRESS horseradish peroxidase (HRP) secondary Ab (Vector Laboratories) for immunohistochemistry staining or Alexa Fluor–labeled secondary Abs (Thermo Fisher Scientific) or Alexa Fluor–conjugated streptavidin (Thermo Fisher Scientific) for immunofluorescence. Antifade Mountant with DAPI (Vector Laboratories) was used as the mounting medium. Immunofluorescence images were captured on a Zeiss LSM 700 confocal microscope (Zeiss). Immunohistochemical staining of human scalp tissue sections was performed as previously described (*6*, *18*).

Human scalp tissue was fixed in 4% paraformaldehyde and was embedded in paraffin after sequential dehydration in ethanol and xylene. Paraffin sections were cut at 6 μm, deparaffinized, and microwaved using heat-induced antigen retrieval in 10 mM tris and 1 mM EDTA (pH 8.0). Tissue sections were then incubated with anti-CD4 (SP35, Abcam), anti-CD8 (SP16, Abcam), anti–IL-7 (PeproTech), or anti–IL-7Rα (LS Bio) overnight at 4°C after blocking with 5% donkey serum (Vector Laboratories). After ImmPRESS HRP secondary Ab (Vector Laboratories) incubation, detection of Ab complexes was followed by incubation with ImmPACT NovaRED Peroxidase (HRP) Substrate (Vector Laboratories). Counterstaining was performed with Mayer's Hematoxylin (Sigma-Aldrich) for 2 min and bluing in Scott's tap water solution.

RNA sequencing and bioinformatic analysis

Total cellular RNA was extracted using the RNeasy Kit (Qiagen) from skin homogenates. RNA quality and quantity were determined using an Agilent BioAnalyzer (Agilent Technologies). mRNA was converted to complementary DNA (cDNA) using random primers and reverse transcriptase. cDNA library construction and RNA sequencing were performed at GENEWIZ. RNA sequencing reads and read quality were performed using STAR Aligner with the corresponding Ensembl 84 reference genomes and FastQC v0.11.2. To visualize the raw similarity or divergence of the gene expression profile of each sample, we used the normalized hit count from each sample to perform unsupervised analyses. The hit counts of each sample were normalized by the DESeq2 package in Bioconductor, which can estimate variance-mean dependence in count data from high-throughput sequencing assays and test for differential expression based on a model using the negative binomial distribution (*56*). Principal components analysis (PCA) was performed with the plotPCA function in DESeq2 to display the overall difference of the gene expression profile in each sample and how similar or dissimilar they are to each other in an unsupervised manner. To visualize the difference in expression in the ALADIN genes (*6*), the normalized hit counts of the ALADIN genes in each sample were plotted as a heatmap using the pheatmap package in Bioconductor. Similarly, the unsupervised hierarchical clustering of the samples was based on their similarity or difference in expression in ALADIN genes, naïve to their treatment.

Quantitative polymerase chain reaction assay

Total RNA was isolated using the RNeasy Kit (Qiagen), and cDNA synthesis was performed using SuperScript III Reverse Transcriptase (Thermo Fisher Scientific). Quantitative polymerase chain reaction (PCR) assays were performed using QuantStudio 7 PCR detection system (Thermo Fisher Scientific), and an SYBR Green

amplification kit (Thermo Fisher Scientific) to determine the expression of mRNA in the skin using the following primers (forward and reverse listed 5′ to 3′): IL-7 (5′-TTCCTCCACTGATCCTTGTTCT-3′ and 5′-AGCAGCTTCCTTTGTATCATCAC-3′), PD-L1 (5′ AGTATGGCAGCAACGTCACG-3′ and 5′-TCCTTTTCCCAGTACACCACTA-3′), PD-L2 (5'CTGCCGATACTGAACCTGAGC-3′ and 5′-GCGGTCAAAATCGCACTCC-3′), and glyceraldehyde-3-phosphate dehydrogenase (GAPDH) (5′-GAAGGTCGGTGTGAACGGA-3′ and 5′-GTTAGTGGGGTCTCGCTCCT-3′). Samples were analyzed in triplicate and normalized to GAPDH.

Statistics

Statistical analyses were performed using the GraphPad Prism 7.0 software. Groups of data were compared using a two-tailed Student's *t* test. Log-rank tests were used to analyze the hair loss or regrowth curves. One-way analysis of variance (ANOVA) was used for mean differences comparison from multiple groups. Data in bar and dot graphs are means ± SD. Significance is indicated as follows: $*P < 0.05$; $**P < 0.01$; $***P < 0.001$; $****P < 0.0001$.

SUPPLEMENTARY MATERIALS

Supplementary material for this article is available at http://advances.sciencemag.org/cgi/content/full/7/14/eabd1866/DC1

View/request a protocol for this paper from *Bio-protocol*.

REFERENCES AND NOTES

1. A. Gilhar, A. Etzioni, R. Paus, Alopecia areata. *N. Engl. J. Med.* **366**, 1515–1525 (2012).
2. A. Gilhar, M. Landau, B. Assy, Y. Ullmann, R. Shalaginov, S. Serafimovich, R. S. Kalish, Transfer of alopecia areata in the human scalp graft/Prkdcscid (SCID) mouse system is characterized by a TH1 response. *Clin. Immunol.* **106**, 181–187 (2003).
3. K. J. McElwee, A. Gilhar, D. J. Tobin, Y. Ramot, J. P. Sundberg, M. Nakamura, M. Bertolini, S. Inui, Y. Tokura, L. E. King Jr., B. Duque-Estrada, A. Tosti, A. Keren, S. Itami, Y. Shoenfeld, A. Zlotogorski, R. Paus, What causes alopecia areata? *Exp. Dermatol.* **22**, 609–626 (2013).
4. R. Paus, B. J. Nickoloff, T. Ito, A 'hairy' privilege. *Trends Immunol.* **26**, 32–40 (2005).
5. L. Petukhova, M. Duvic, M. Hordinsky, D. Norris, V. Price, Y. Shimomura, H. Kim, P. Singh, A. Lee, W. V. Chen, K. C. Meyer, R. Paus, C. A. Jahoda, C. I. Amos, P. K. Gregersen, A. M. Christiano, Genome-wide association study in alopecia areata implicates both innate and adaptive immunity. *Nature* **466**, 113–117 (2010).
6. L. Xing, Z. Dai, A. Jabbari, J. E. Cerise, C. A. Higgins, W. Gong, A. de Jong, S. Harel, G. M. DeStefano, L. Rothman, P. Singh, L. Petukhova, J. Mackay-Wiggan, A. M. Christiano, R. Clynes, Alopecia areata is driven by cytotoxic T lymphocytes and is reversed by JAK inhibition. *Nat. Med.* **20**, 1043–1049 (2014).
7. T. J. Fry, C. L. Mackall, The many faces of IL-7: From lymphopoiesis to peripheral T cell maintenance. *J. Immunol.* **174**, 6571–6576 (2005).
8. H. Dooms, Interleukin-7: Fuel for the autoimmune attack. *J. Autoimmun.* **45**, 40–48 (2013).
9. F. Carrette, C. D. Surh, IL-7 signaling and CD127 receptor regulation in the control of T cell homeostasis. *Semin. Immunol.* **24**, 209–217 (2012).
10. L. F. Lee, R. Axtell, G. H. Tu, K. Logronio, J. Dilley, J. Yu, M. Rickert, B. Han, W. Evering, M. G. Walker, J. Shi, B. A. de Jong, J. Killestein, C. H. Polman, L. Steinman, J. C. Lin, IL-7 promotes T_H1 development and serum IL-7 predicts clinical response to interferon-β in multiple sclerosis. *Sci. Transl. Med.* **3**, 93ra68 (2011).
11. C. Penaranda, W. Kuswanto, J. Hofmann, R. Kenefeck, P. Narendran, L. S. Walker, J. A. Bluestone, A. K. Abbas, H. Dooms, IL-7 receptor blockade reverses autoimmune diabetes by promoting inhibition of effector/memory T cells. *Proc. Natl. Acad. Sci. U.S.A.* **109**, 12668–12673 (2012).
12. S. A. Hartgring, C. R. Willis, D. Alcorn, L. J. Nelson, J. W. Bijlsma, F. P. Lafeber, J. A. van Roon, Blockade of the interleukin-7 receptor inhibits collagen-induced arthritis and is associated with reduction of T cell activity and proinflammatory mediators. *Arthritis Rheum.* **62**, 2716–2725 (2010).
13. A. Gilhar, R. Paus, R. S. Kalish, Lymphocytes, neuropeptides, and genes involved in alopecia areata. *J. Clin. Invest.* **117**, 2019–2027 (2007).
14. T. Adachi, T. Kobayashi, E. Sugihara, T. Yamada, K. Ikuta, S. Pittaluga, H. Saya, M. Amagai, K. Nagao, Hair follicle-derived IL-7 and IL-15 mediate skin-resident memory T cell homeostasis and lymphoma. *Nat. Med.* **21**, 1272–1279 (2015).
15. T. Hara, S. Shitara, K. Imai, H. Miyachi, S. Kitano, H. Yao, S. Tani-ichi, K. Ikuta, Identification of IL-7-producing cells in primary and secondary lymphoid organs using IL-7-GFP knock-in mice. *J. Immunol.* **189**, 1577–1584 (2012).
16. S. Shalapour, K. Deiser, O. Sercan, J. Tuckermann, K. Minnich, G. Willimsky, T. Blankenstein, G. J. Hammerling, B. Arnold, T. Schuler, Commensal microflora and interferon-gamma promote steady-state interleukin-7 production in vivo. *Eur. J. Immunol.* **40**, 2391–2400 (2010).
17. R. C. Axtell, C. Raman, Janus-like effects of type I interferon in autoimmune diseases. *Immunol. Rev.* **248**, 23–35 (2012).
18. Z. Dai, L. Xing, J. Cerise, E. H. Wang, A. Jabbari, A. de Jong, L. Petukhova, A. M. Christiano, R. Clynes, CXCR3 blockade inhibits T cell migration into the skin and prevents development of alopecia areata. *J. Immunol.* **197**, 1089–1099 (2016).
19. R. Zeng, R. Spolski, S. E. Finkelstein, S. Oh, P. E. Kovanen, C. S. Hinrichs, C. A. Pise-Masison, M. F. Radonovich, J. N. Brady, N. P. Restifo, J. A. Berzofsky, W. J. Leonard, Synergy of IL-21 and IL-15 in regulating CD8+ T cell expansion and function. *J. Exp. Med.* **201**, 139–148 (2005).
20. C. E. Martin, E. M. van Leeuwen, S. J. Im, D. C. Roopenian, Y.-C. Sung, C. D. Surh, IL-7/anti-IL-7 mAb complexes augment cytokine potency in mice through association with IgG-Fc and by competition with IL-7R. *Blood* **121**, 4484–4492 (2013).
21. C. A. Arbelaez, S. Glatigny, R. Duhen, G. Eberl, M. Oukka, E. Bettelli, IL-7/IL-7 receptor signaling differentially affects effector CD4+ T cell subsets involved in experimental autoimmune encephalomyelitis. *J. Immunol.* **195**, 1974–1983 (2015).
22. J. O. Jin, T. Kawai, S. Cha, Q. Yu, Interleukin-7 enhances the Th1 response to promote the development of Sjögren's syndrome-like autoimmune exocrinopathy in mice. *Arthritis Rheum.* **65**, 2132–2142 (2013).
23. G. Varricchi, A. Pecoraro, G. Marone, G. Criscuolo, G. Spadaro, A. Genovese, G. Marone, Thymic stromal lymphopoietin isoforms, inflammatory disorders, and cancer. *Front. Immunol.* **9**, 1595 (2018).
24. C. L. Sokol, G. M. Barton, A. G. Farr, R. Medzhitov, A mechanism for the initiation of allergen-induced T helper type 2 responses. *Nat. Immunol.* **9**, 310–318 (2008).
25. M. L. Bettini, M. Bettini, D. A. Vignali, T-cell receptor retrogenic mice: A rapid, flexible alternative to T-cell receptor transgenic mice. *Immunology* **136**, 265–272 (2012).
26. R. Alli, P. Nguyen, K. Boyd, J. P. Sundberg, T. L. Geiger, A mouse model of clonal $CD8^+$ T lymphocyte-mediated alopecia areata progressing to alopecia universalis. *J. Immunol.* **188**, 477–486 (2012).
27. K. J. McElwee, P. Freyschmidt-Paul, R. Hoffmann, S. Kissling, S. Hummel, M. Vitacolonna, M. Zoller, Transfer of $CD8^+$ cells induces localized hair loss whereas CD4(+)/CD25(−) cells promote systemic alopecia areata and CD4(+)/CD25(+) cells blockade disease onset in the C3H/HeJ mouse model. *J. Invest. Dermatol.* **124**, 947–957 (2005).
28. S. Sakaguchi, T. Yamaguchi, T. Nomura, M. Ono, Regulatory T cells and immune tolerance. *Cell* **133**, 775–787 (2008).
29. T. Okazaki, T. Honjo, The PD-1-PD-L pathway in immunological tolerance. *Trends Immunol.* **27**, 195–201 (2006).
30. T. Yamaguchi, K. Hirota, K. Nagahama, K. Ohkawa, T. Takahashi, T. Nomura, S. Sakaguchi, Control of immune responses by antigen-specific regulatory T cells expressing the folate receptor. *Immunity* **27**, 145–159 (2007).
31. S. C. Liang, M. Moskalenko, M. Van Roey, K. Jooss, Depletion of regulatory T cells by targeting folate receptor 4 enhances the potency of a GM-CSF-secreting tumor cell immunotherapy. *Clin. Immunol.* **148**, 287–298 (2013).
32. J. D. Fontenot, J. P. Rasmussen, M. A. Gavin, A. Y. Rudensky, A function for interleukin 2 in Foxp3-expressing regulatory T cells. *Nat. Immunol.* **6**, 1142–1151 (2005).
33. A. Sharabi, M. G. Tsokos, Y. Ding, T. R. Malek, D. Klatzmann, G. C. Tsokos, Regulatory T cells in the treatment of disease. *Nat. Rev. Drug Discov.* **17**, 823–844 (2018).
34. L. Barron, H. Dooms, K. K. Hoyer, W. Kuswanto, J. Hofmann, W. E. O'Gorman, A. K. Abbas, Cutting edge: Mechanisms of IL-2-dependent maintenance of functional regulatory T cells. *J. Immunol.* **185**, 6426–6430 (2010).
35. F. Depis, H. K. Kwon, D. Mathis, C. Benoist, Unstable FoxP3+ T regulatory cells in NZW mice. *Proc. Natl. Acad. Sci. U.S.A.* **113**, 1345–1350 (2016).
36. D. Klatzmann, A. K. Abbas, The promise of low-dose interleukin-2 therapy for autoimmune and inflammatory diseases. *Nat. Rev. Immunol.* **15**, 283–294 (2015).
37. E. Castela, F. Le Duff, C. Butori, M. Ticchioni, P. Hofman, P. Bahadoran, J. P. Lacour, T. Passeron, Effects of low-dose recombinant interleukin 2 to promote T-regulatory cells in alopecia areata. *JAMA Dermatol.* **150**, 748–751 (2014).
38. C. Schiering, T. Krausgruber, A. Chomka, A. Frohlich, K. Adelmann, E. A. Wohlfert, J. Pott, T. Griseri, J. Bollrath, A. N. Hegazy, O. J. Harrison, B. M. J. Owens, M. Lohning, Y. Belkaid, P. G. Fallon, F. Powrie, The alarmin IL-33 promotes regulatory T-cell function in the intestine. *Nature* **513**, 564–568 (2014).

39. X. Yuan, Y. Dong, N. Tsurushita, J. Y. Tso, W. Fu, CD122 blockade restores immunological tolerance in autoimmune type 1 diabetes via multiple mechanisms. *JCI Insight* **3**, 96600 (2018).
40. R. I. Mazzucchelli, A. Riva, S. K. Durum, The human IL-7 receptor gene: Deletions, polymorphisms and mutations. *Semin. Immunol.* **24**, 225–230 (2012).
41. T. Calzascia, M. Pellegrini, A. Lin, K. M. Garza, A. R. Elford, A. Shahinian, P. S. Ohashi, T. W. Mak, CD4 T cells, lymphopenia, and IL-7 in a multistep pathway to autoimmunity. *Proc. Natl. Acad. Sci. U.S.A.* **105**, 2999–3004 (2008).
42. A. J. Papadopoulos, R. A. Schwartz, C. K. Janniger, Alopecia areata. Pathogenesis, diagnosis, and therapy. *Am. J. Clin. Dermatol.* **1**, 101–105 (2000).
43. A. Alkhalifah, A. Alsantali, E. Wang, K. J. McElwee, J. Shapiro, Alopecia areata update: Part I. Clinical picture, histopathology, and pathogenesis. *J. Am. Acad. Dermatol.* **62**, 177–188 (2010).
44. M. E. Weinblatt, J. M. Kremer, A. D. Bankhurst, K. J. Bulpitt, R. M. Fleischmann, R. I. Fox, C. G. Jackson, M. Lange, D. J. Burge, A trial of etanercept, a recombinant tumor necrosis factor receptor:Fc fusion protein, in patients with rheumatoid arthritis receiving methotrexate. *N. Engl. J. Med.* **340**, 253–259 (1999).
45. P. J. Mease, I. B. McInnes, B. Kirkham, A. Kavanaugh, P. Rahman, D. van der Heijde, R. Landewe, P. Nash, L. Pricop, J. Yuan, H. B. Richards, S. Mpofu; FUTURE 1 Study Group, Secukinumab inhibition of interleukin-17A in patients with psoriatic arthritis. *N. Engl. J. Med.* **373**, 1329–1339 (2015).
46. D. A. Cronkite, T. M. Strutt, The regulation of inflammation by innate and adaptive lymphocytes. *J. Immunol. Res.* **2018**, 1467538 (2018).
47. P. Freyschmidt-Paul, K. J. McElwee, R. Hoffmann, J. P. Sundberg, M. Vitacolonna, S. Kissling, M. Zoller, Interferon-γ-deficient mice are resistant to the development of alopecia areata. *Br. J. Dermatol.* **155**, 515–521 (2006).
48. K. Ariizumi, Y. Meng, P. R. Bergstresser, A. Takashima, IFN-gamma-dependent IL-7 gene regulation in keratinocytes. *J. Immunol.* **154**, 6031–6039 (1995).
49. L. Belarif, R. Danger, L. Kermarrec, V. Nerriere-Daguin, S. Pengam, T. Durand, C. Mary, E. Kerdreux, V. Gauttier, A. Kucik, V. Thepenier, J. C. Martin, C. Chang, A. Rahman, N. S. Guen, C. Braudeau, A. Abidi, G. David, F. Malard, C. Takoudju, B. Martinet, N. Gerard, I. Neveu, M. Neunlist, E. Coron, T. T. MacDonald, P. Desreumaux, H. L. Mai, S. Le Bas-Bernardet, J. F. Mosnier, M. Merad, R. Josien, S. Brouard, J. P. Soulillou, G. Blancho, A. Bourreille, P. Naveilhan, B. Vanhove, N. Poirier, IL-7 receptor influences anti-TNF responsiveness and T cell gut homing in inflammatory bowel disease. *J. Clin. Invest.* **129**, 1910–1925 (2019).
50. L. Belarif, C. Mary, L. Jacquemont, H. L. Mai, R. Danger, J. Hervouet, D. Minault, V. Thepenier, V. Nerriere-Daguin, E. Nguyen, S. Pengam, E. Largy, A. Delobel, B. Martinet, S. Le Bas-Bernardet, S. Brouard, J. P. Soulillou, N. Degauque, G. Blancho, B. Vanhove, N. Poirier, IL-7 receptor blockade blunts antigen-specific memory T cell responses and chronic inflammation in primates. *Nat. Commun.* **9**, 4483 (2018).
51. L. M. Francisco, P. T. Sage, A. H. Sharpe, The PD-1 pathway in tolerance and autoimmunity. *Immunol. Rev.* **236**, 219–242 (2010).
52. H. L. Mai, F. Boeffard, J. Longis, R. Danger, B. Martinet, F. Haspot, B. Vanhove, S. Brouard, J. P. Soulillou, IL-7 receptor blockade following T cell depletion promotes long-term allograft survival. *J. Clin. Invest.* **124**, 1723–1733 (2014).
53. A. Visperas, D. A. Vignali, Are regulatory T cells defective in type 1 diabetes and can we fix them? *J. Immunol.* **197**, 3762–3770 (2016).
54. B. Griesenauer, S. Paczesny, The ST2/IL-33 axis in immune cells during inflammatory diseases. *Front. Immunol.* **8**, 475 (2017).
55. A. N. McMurchy, M. K. Levings, Suppression assays with human T regulatory cells: A technical guide. *Eur. J. Immunol.* **42**, 27–34 (2012).
56. M. I. Love, W. Huber, S. Anders, Moderated estimation of fold change and dispersion for RNA-seq data with DESeq2. *Genome Biol.* **15**, 550 (2014).

Acknowledgments: We thank E. Chang, J. Huang, M. Zhang, and W. Zeng for expert assistance in the laboratory. **Funding:** This study was supported by NIH/NIAMS grant P50AR070588 Alopecia Areata Center for Research Translation (AACORT) and the Locks of Love Foundation. Z.D. is a recipient of a mentored young investigator grant award from National Alopecia Areata Foundation and a K01AR070291 award from NIH/NIAMS. E.Y.L. is supported by the Medical Scientist Training Program at Columbia University Irving Medical Center (T32GM007367). We appreciate the support of the Skin Disease Research Center in the Department of Dermatology (P30AR69632) at Columbia University. **Author contributions:** Z.D. led and performed experiments and analyzed data. E.H.C.W., L.P., Y.C., and E.Y.L. performed experiments and analyzed data. All authors provided critical review of the manuscript. Z.D. and A.M.C. analyzed data and wrote the manuscript. A.M.C. conceived and supervised the study and provided funding. **Competing interests:** The authors declare that they have no potential, perceived, or real conflict of interest regarding the content of this manuscript. **Data and materials availability:** All data needed to evaluate the conclusions in the paper are present in the paper and/or the Supplementary Materials. Additional data related to this paper may be requested from the authors.

Submitted 5 June 2020
Accepted 16 February 2021
Published 2 April 2021
10.1126/sciadv.abd1866

Citation: Z. Dai, E. H. C. Wang, L. Petukhova, Y. Chang, E. Y. Lee, A. M. Christiano, Blockade of IL-7 signaling suppresses inflammatory responses and reverses alopecia areata in C3H/HeJ mice. *Sci. Adv.* **7**, eabd1866 (2021).